

DESY 13-017
Edinburgh 2013/01
LTH 969
February 2013

Nucleon axial charge and pion decay constant from two-flavor lattice QCD

R. Horsley¹, Y. Nakamura², A. Nobile³, P.E.L. Rakow⁴,
G. Schierholz⁵ and J.M. Zanotti⁶

¹ *School of Physics and Astronomy,
University of Edinburgh,
Edinburgh EH9 3JZ, United Kingdom*

² *RIKEN Advanced Institute for Computational Science,
Kobe, Hyogo 650-0047, Japan*

³ *JSC, Forschungszentrum Jülich,
52425 Jülich, Germany*

⁴ *Theoretical Physics Division,
Department of Mathematical Sciences,
University of Liverpool,
Liverpool L69 3BX, United Kingdom*

⁵ *Deutsches Elektronen-Synchrotron DESY,
22603 Hamburg, Germany*

⁶ *CSSM, School of Chemistry and Physics,
University of Adelaide,
Adelaide SA 5005, Australia*

– QCDSF Collaboration –

Abstract

The axial charge of the nucleon g_A and the pion decay constant f_π are computed in two-flavor lattice QCD. The simulations are carried out on lattices of various volumes and lattice spacings. Results are reported for pion masses as low as $m_\pi = 130$ MeV. The volume dependence of g_A and f_π can be understood quantitatively in terms of lattice ChPT. At the physical pion mass we find $g_A = 1.24(4)$ and $f_\pi = 89 \pm 1.1 \pm 1.8$ MeV, using $r_0 = 0.50(1)$ fm to set the scale, in good agreement with experiment. As a by-product we obtain the low-energy constant $\bar{l}_4 = 4.2(1)$.

PACS numbers: 12.38.Gc

I. INTRODUCTION

The axial charge g_A of the nucleon is a fundamental measure of nucleon structure. While g_A has been known accurately for many years from neutron β decays, a calculation of g_A from first principles still presents a significant challenge. Present lattice calculations [1–5], except perhaps [4], underestimate the experimental value by a large amount. The resolution of this problem is of great importance to any further calculation of hadron structure.

Lattice calculations of g_A are in many ways connected to calculations of the pion decay constant f_π . Both quantities involve the axial vector current, which is not conserved and thus needs to be renormalized. Though it is standard practice nowadays to compute the renormalization constant nonperturbatively [6, 7], some scope of uncertainty remains [8]. Another common feature is that g_A and f_π seem to be affected by large finite size corrections, in particular at small pion masses, which to leading order ChEFT and ChPT [9–11] appear to be the same in both cases. This led us to suggest to determine g_A from the ratio g_A/f_π . First results [12] looked indeed encouraging.

In this paper we present our results on g_A and f_π for two flavors of nonperturbatively $O(a)$ improved Wilson fermions and Wilson plaquette action [13]. This includes simulations about the physical pion mass and on various lattice volumes and at various lattice spacings. The main focus is on finite size corrections, and the extrapolation of g_A and f_π to the thermodynamic limit at the physical point.

II. LATTICE SIMULATION

Our lattice ensembles are listed in Table I. The pion masses and the chirally extrapolated values of r_0/a are taken from our preceding paper [13] on the nucleon mass and sigma term. The Sommer parameter was found to be $r_0 = 0.50(1)$ fm, which we will use to set the scale throughout this paper. The ensembles cover three β values, $\beta = 5.25, 5.29$ and 5.40 , with lattice spacings $a = 0.076, 0.071$ and 0.060 fm.

We employ the improved axial vector current

$$\mathcal{A}_\mu(x) = \bar{q}(x)\gamma_\mu\gamma_5q(x) + ac_A\partial_\mu\bar{q}(x)\gamma_5q(x), \quad (1)$$

where c_A is taken from [14]. The improvement term does not contribute to forward matrix elements, but it will contribute to f_π . The calculation of g_A follows [10, 15, 16] with one

β	κ	Volume	am_π	g_A	af_π	r_0/a
5.25	0.13460	$16^3 \times 32$	0.4932(10)	1.442(13)	0.0886(8)	6.603(53)
5.25	0.13520	$16^3 \times 32$	0.3821(13)	1.438(20)	0.0756(8)	
5.25	0.13575	$24^3 \times 48$	0.2556(5)	1.456(10)	0.0635(5)	
5.25	0.13600	$24^3 \times 48$	0.1840(7)	1.412(18)	0.0550(4)	
5.25	0.13620	$32^3 \times 64$	0.0997(11)	1.368(51)	0.0439(6)	
5.29	0.13400	$16^3 \times 32$	0.5767(11)	1.437(12)	0.0936(9)	7.004(54)
5.29	0.13500	$16^3 \times 32$	0.4206(9)	1.409(12)	0.0778(5)	
5.29	0.13550	$12^3 \times 32$	0.3605(32)	1.181(60)	0.0568(8)	
5.29	0.13550	$16^3 \times 32$	0.3325(14)	1.371(20)	0.0675(6)	
5.29	0.13550	$24^3 \times 48$	0.3270(6)	1.459(11)	0.0689(7)	
5.29	0.13590	$12^3 \times 32$	0.3369(62)	0.967(105)	0.0345(9)	
5.29	0.13590	$16^3 \times 32$	0.2518(15)	1.271(32)	0.0559(5)	
5.29	0.13590	$24^3 \times 48$	0.2395(5)	1.426(7)	0.0588(3)	
5.29	0.13620	$24^3 \times 48$	0.1552(6)	1.334(18)	0.0478(3)	
5.29	0.13632	$24^3 \times 48$	0.1112(9)	1.271(67)	0.0398(4)	
5.29	0.13632	$32^3 \times 64$	0.1070(5)	1.409(24)	0.0440(3)	
5.29	0.13632	$40^3 \times 64$	0.1050(3)	1.439(17)	0.0445(3)	
5.29	0.13640	$40^3 \times 64$	0.0660(8)	1.363(105)	0.0375(5)	
5.29	0.13640	$48^3 \times 64$	0.0570(7)	1.572(52)	0.0408(11)	
5.40	0.13500	$24^3 \times 48$	0.4030(4)	1.474(7)	0.0691(5)	8.285(74)
5.40	0.13560	$24^3 \times 48$	0.3123(7)	1.451(11)	0.0620(5)	
5.40	0.13610	$24^3 \times 48$	0.2208(7)	1.410(20)	0.0513(4)	
5.40	0.13625	$24^3 \times 48$	0.1902(6)	1.377(20)	0.0470(3)	
5.40	0.13640	$24^3 \times 48$	0.1538(10)	1.261(34)	0.0419(4)	
5.40	0.13640	$32^3 \times 64$	0.1505(5)	1.402(17)	0.0442(4)	
5.40	0.13660	$32^3 \times 64$	0.0845(6)	1.206(79)	0.0342(4)	
5.40	0.13660	$48^3 \times 64$	0.0797(3)	1.403(29)	0.0362(3)	

TABLE I: Parameters of our lattice data sets, together with the pion mass, the bare axial charge and the pion decay constant. Also listed are the chirally extrapolated values of r_0/a .

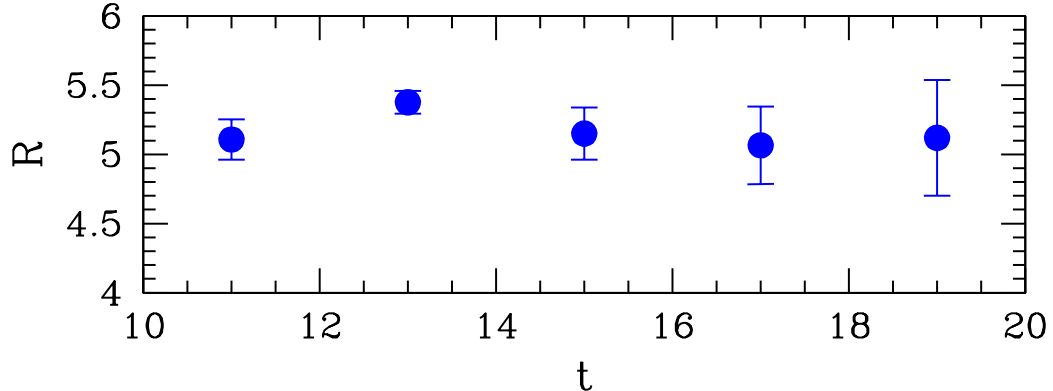


FIG. 1: The ratio R as a function of the source-sink time separation t on the $24^3 \times 48$ lattice at $\beta = 5.29$, $\kappa = 0.13590$.

exception, namely that on the $48^3 \times 64$ lattice at $\beta = 5.29$, $\kappa = 0.13640$ we have employed Wuppertal smearing instead of Jacobi smearing. It involves computing the ratio of two- and three-point functions

$$R_{\alpha\beta}(t, \tau) = \frac{\langle N_{\alpha}(t) \mathcal{A}_{\mu}(\tau) \bar{N}_{\beta}(0) \rangle}{\langle N(t) \bar{N}(0) \rangle}, \quad (2)$$

\bar{N} and N being the nucleon creation and annihilation operators at zero momentum. Any smearing of the source (at time 0) and sink operators (at time t) is cancelled in this ratio. For $\beta = 5.4$ we use $t = 17$, while the lightest two ensembles at $\beta = 5.29$, $\kappa = 0.13640$ and $\kappa = 0.13632$, use $t = 15$. All other ensembles use $t = 13$.

In [4] it has been argued that contributions from excited states might be the reason for g_A falling short of the experimental value. To investigate this scenario, we have performed additional simulations on the $24^3 \times 48$ lattice at $\beta = 5.29$, $\kappa = 0.13590$ with a large range of different source-sink separations, $t = 11, \dots, 19$, albeit with somewhat lower statistics than our reference point at $t = 13$. In Fig. 1 we show the ratio R for various time separations t between source and sink. If true, we should find a larger value at separations $t > 13$. However, we do not see any systematic deviation of R from our result at $t = 13$ within the error bars, not even for $t = 11$. This provides us with confidence that our choices of t are sufficient with our choice of source and sink smearing. Similar conclusions were found in [3].

Our smearing parameters are tuned to give a *rms* radius of ≈ 0.5 fm, which is about half the radius of the nucleon. For this level of smearing no further improvement of the extracted

result for g_A was found by employing variational techniques [17], which systematically separate excited states out from the ground state at source and sink.

The calculation of f_π follows [18]. We use the notation employed in ChPT, with the experimental value $f_{\pi^+} = 92.2 \text{ MeV}$. Our final results for the bare quantities, g_A and af_π , on all of our ensembles are given in Table I.

III. FINITE SIZE CORRECTIONS

Let us first consider the finite size corrections to g_A . Utilizing the (nonrelativistic) small scale expansion (SSE) of the ChEFT, including pion, nucleon (N) and $\Delta(1232)$ degrees of freedom, we obtain to $O(\epsilon^3)$ [10]

$$\frac{g_A(L) - g_A(\infty)}{g_A(\infty)} = -\frac{m_\pi^2}{4\pi^2 f_0^2} \sum_{\substack{\mathbf{n} \\ |\mathbf{n}| \neq 0}} \frac{K_1(\lambda|\mathbf{n}|)}{\lambda|\mathbf{n}|} + \Delta(L) \quad (3)$$

with

$$\begin{aligned} \Delta(L) = & \frac{g_A^2 m_\pi^2}{6\pi^2 f_0^2} \sum_{\substack{\mathbf{n} \\ |\mathbf{n}| \neq 0}} \left[K_0(\lambda|\mathbf{n}|) - \frac{K_1(\lambda|\mathbf{n}|)}{\lambda|\mathbf{n}|} \right] \\ & + \frac{25c_A^2 g_1}{81\pi^2 g_A f_0^2} \int_0^\infty dy y \sum_{\substack{\mathbf{n} \\ |\mathbf{n}| \neq 0}} \left[K_0(\lambda(y)|\mathbf{n}|) - \frac{\lambda(y)|\mathbf{n}|}{3} K_1(\lambda(y)|\mathbf{n}|) \right] \\ & - \frac{c_A^2}{\pi^2 f_0^2} \int_0^\infty dy y \sum_{\substack{\mathbf{n} \\ |\mathbf{n}| \neq 0}} \left[K_0(\lambda(y)|\mathbf{n}|) - \frac{\lambda(y)|\mathbf{n}|}{3} K_1(\lambda(y)|\mathbf{n}|) \right] \\ & + \frac{8c_A^2 m_\pi^2}{27\pi^2 f_0^2 \Delta_0} \int_0^\infty dy \sum_{\substack{\mathbf{n} \\ |\mathbf{n}| \neq 0}} \left(\frac{\lambda(y)}{\lambda} \right)^2 \left[K_0(\lambda(y)|\mathbf{n}|) - \frac{K_1(\lambda(y)|\mathbf{n}|)}{\lambda(y)|\mathbf{n}|} \right] \\ & - \frac{4c_A^2 m_\pi^3}{27\pi f_0^2 \Delta_0} \sum_{\substack{\mathbf{n} \\ |\mathbf{n}| \neq 0}} \frac{e^{-\lambda|\mathbf{n}|}}{\lambda|\mathbf{n}|}, \end{aligned} \quad (4)$$

where $\lambda = m_\pi L$ and $\lambda(y) = f(m_\pi, y)L$ with $f(m_\pi, y) = \sqrt{m_\pi^2 + y^2 + 2y\Delta_0}$, Δ_0 being the $\Delta - N$ mass difference. K_0 and K_1 denote the modified Bessel functions, and c_A and g_1 are the leading axial ΔN and $\Delta\Delta$ couplings. The parameter c_A should not be confused with the improvement coefficient c_A in eq. (1).

The second term in eq. (3), $\Delta(L)$, receives contributions from chiral loops, which renormalize the axial charge and act on intermediate Δ baryons [10]. It turns out that the various contributions to $\Delta(L)$ effectively cancel each other over a wide range of λ values. This has

been noticed by the authors of [19] as well. To state an example, let us consider the $48^3 \times 64$ lattice at $\beta = 5.29$, $\kappa = 0.13640$. This lattice has the lowest pion mass and is especially important for our final conclusions. Taking $c_A = 1.5$ from [20] and $g_1 = 2.16$ from $SU(6)$, we find -0.044 for the total contribution, but only $+0.001$ for $\Delta(L)$. We thus may assume

$$\frac{g_A(L) - g_A(\infty)}{g_A(\infty)} = -\frac{m_\pi^2}{4\pi^2 f_0^2} \sum_{\substack{\mathbf{n} \\ |\mathbf{n}| \neq 0}} \frac{K_1(\lambda|\mathbf{n}|)}{\lambda|\mathbf{n}|}. \quad (5)$$

The finite size corrections to f_π have been computed in [11] within the context of ChPT. To NLO ($\propto m_\pi^2$) the outcome is

$$\frac{f_\pi(L) - f_\pi(\infty)}{f_\pi(\infty)} = -\frac{m_\pi^2}{4\pi^2 f_0^2} \sum_{\substack{\mathbf{n} \\ |\mathbf{n}| \neq 0}} \frac{K_1(\lambda|\mathbf{n}|)}{\lambda|\mathbf{n}|}. \quad (6)$$

The NNLO corrections are found to be very small and, thus, can safely be neglected.

This finally shows that the leading finite size corrections to g_A and f_π are basically the same and will cancel in the ratio g_A/f_π . Once f_0 , the pion decay constant in the chiral limit, has been fixed, expressions (5) and (6) have only one free parameter, $g_A(\infty)$ and $f_\pi(\infty)$, respectively.

The NLO correction to the pion mass reads [11]

$$\frac{m_\pi(L) - m_\pi(\infty)}{m_\pi(\infty)} = \frac{m_\pi^2}{16\pi^2 f_0^2} \sum_{\substack{\mathbf{n} \\ |\mathbf{n}| \neq 0}} \frac{K_1(\lambda|\mathbf{n}|)}{\lambda|\mathbf{n}|}. \quad (7)$$

At smaller values of $m_\pi L$, $m_\pi L \lesssim 3$, this expression alone cannot describe the observed finite size effects [13]. That is not surprising, since in a finite spatial box chiral symmetry does not break down spontaneously. This is because giving the system enough time it will rotate through all vacua. This results in a mass gap at vanishing quark masses [21–23],

$$m_{\pi \text{ res}} = \frac{3}{2f_0^2 L^3 (1 + \Delta)} \quad (8)$$

with

$$\begin{aligned} \Delta = & \frac{2}{f_0^2 L^2} 0.2257849591 \\ & + \frac{1}{f_0^4 L^4} \left[0.088431628 - \frac{0.8375369106}{3\pi^2} \left(\frac{1}{4} \ln(\Lambda_1^2 L^2) + \ln(\Lambda_2^2 L^2) \right) \right], \end{aligned} \quad (9)$$

where Λ_i are the intrinsic scale parameters of the low-energy constants $\bar{l}_i = \ln(\Lambda_i^2/m_{\pi \text{ phys}}^2)$ [24], with $m_{\pi \text{ phys}}$ being the physical pion mass. In [25] we found that the

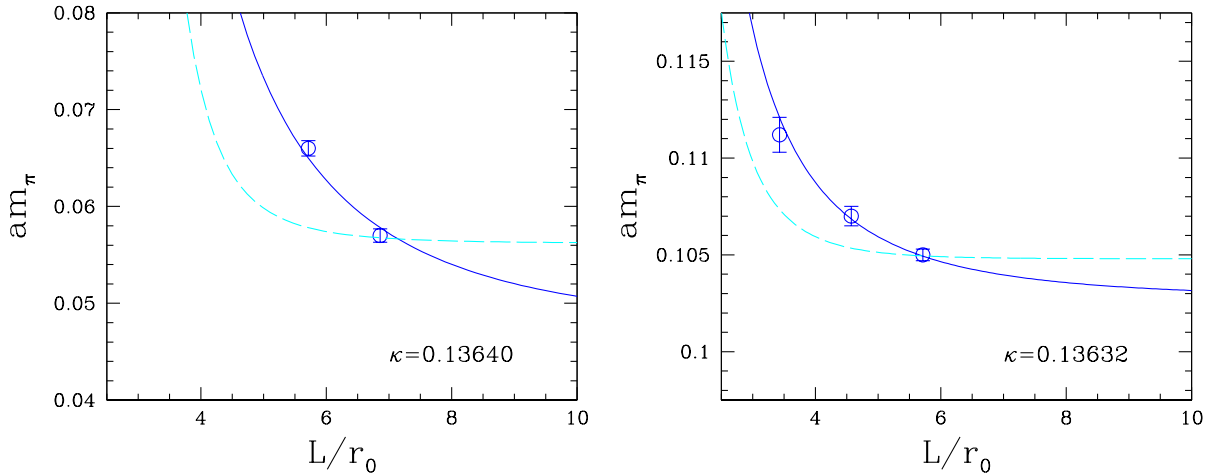


FIG. 2: The pion mass am_π as a function of lattice size for two ensembles at $\beta = 5.29$. The solid line shows a fit of eq. (10) to the data. The dashed line shows the NLO result, eq. (7), fitted to the smallest mass point.

pion mass extrapolates indeed to a finite value in the chiral limit, in good agreement with the expected result (8). This also has an effect on m_π in the region of small, but nonvanishing, quark masses [25]. We thus expect the finite size correction to be effectively given by

$$m_\pi(L) = m_\pi(\infty) + \frac{m_\pi^3}{16\pi^2 f_0^2} \sum_{\substack{\mathbf{n} \\ |\mathbf{n}| \neq 0}} \frac{K_1(\lambda|\mathbf{n}|)}{\lambda|\mathbf{n}|} + \frac{3c(m_\pi)}{2f_0^2 L^3(1+\Delta)} \quad (10)$$

with the parameter $c(m_\pi)$ rapidly dropping to zero at larger pion masses.

IV. EXTRAPOLATION TO INFINITE VOLUME

In the following fits we take $f_0 = 86$ MeV [26]. There is some freedom in the value of the pion mass m_π to take in eqs. (5), (6) and (10). We choose $m_\pi = m_\pi(\infty)$ in λ , $\lambda(y)$ and $c(m_\pi)$, and $m_\pi = m_\pi(L)$ otherwise.

Let us first consider the pion mass. In Fig. 2 we show the fits of eq. (10) to m_π for two of our lattice ensembles. The corrections to m_π are well described by this equation. Apart from $m_\pi(\infty)$, we have one free parameter, $c(m_\pi)$, only. Equally good fits are obtained for $\beta = 5.40$, $\kappa = 0.13660$ and 0.13640 . The parameter $c(m_\pi)$ is found to vanish with a large inverse power of the pion mass. The finite size corrections predicted by the NLO expression

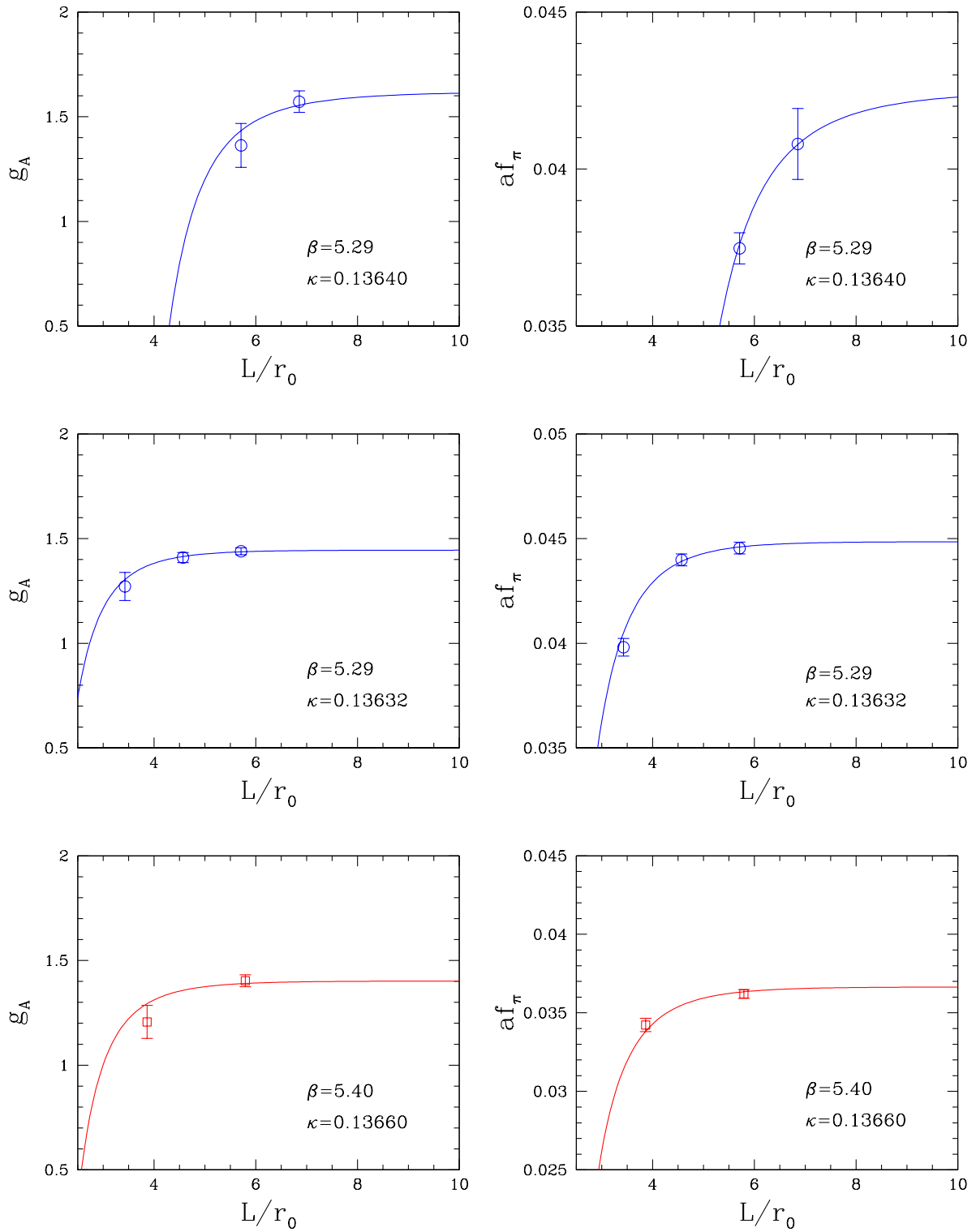


FIG. 3: The bare axial charge g_A and the bare pion decay constant af_π as a function of the spatial extent of the lattice, together with the leading order finite size corrections of eqs. (5) and (6).

(7), on the other hand, are nowhere near as big as the effect shown by the data. In Table II we list our final pion masses. Our lowest mass turns out to be $m_\pi = 130(5)$ MeV.

Let us now turn to the axial charge and the pion decay constant. In Fig. 3 we show the fits of eqs. (5) and (6) to g_A and af_π , respectively, for our three lowest pion masses. It shows that the finite size effects are well described by the leading order formulae. The corrections are large, in particular at the physical pion mass, displayed by the top two figures. On the $L = 3$ fm lattice the corrections are of the order of 10% still.

To obtain continuum numbers, we need to renormalize the axial vector current. That reads

$$\mathcal{A}_\mu^R = Z_A (1 + b_A am_q) \mathcal{A}_\mu. \quad (11)$$

The coefficient b_A is required to maintain $O(a)$ improvement for nonvanishing quark masses m_q as well. The renormalization constant Z_A has been computed nonperturbatively in [7], employing the Rome-Southampton method [6], with the result

β	5.25	5.29	5.40	(12)
Z_A	0.760(1)	0.764(1)	0.777(1)	

The coefficient b_A is only known perturbatively [27], i.e.

$$b_A = 1 + 0.1522 g^2. \quad (13)$$

We denote the renormalized axial charge and pion decay constant by g_A^R and f_π^R , respectively.

In Table II we give our extrapolated numbers. For pion masses $m_\pi \leq 300$ MeV we demand that we have at least two lattice volumes to ensure a controlled extrapolation. This excludes the point at $\beta = 5.25$, $\kappa = 0.13620$ with pion mass $m_\pi \approx 250$ MeV.

V. FINAL RESULTS AND DISCUSSION

Our results for g_A^R are plotted in Fig. 4. Since after finite volume corrections our lightest pion mass is 130 MeV, no extrapolation is required. Instead, we quote our result at our lightest pion mass, namely

$$g_A^R = 1.24 \pm 0.04, \quad (14)$$

in good agreement with the experimental value. It turns out that g_A^R hovers around ≈ 1.1 for $m_\pi \gtrsim 250$ MeV, a feature it shares with most other lattice calculations [5]. Only on the

β	κ	m_π [MeV]	g_A^R	f_π^R [MeV]
5.25	0.13600	479(2)	1.07(1)	108.9(0.8)
5.29	0.13620	426(2)	1.05(2)	103.6(0.6)
5.29	0.13632	284(2)	1.10(2)	94.7(0.6)
5.29	0.13640	130(5)	1.24(4)	89.7(1.5)
5.40	0.13640	492(2)	1.09(1)	112.3(0.9)
5.40	0.13660	253(2)	1.09(2)	93.0(0.7)

TABLE II: The pion mass and the renormalized axial coupling and pion decay constant extrapolated to the infinite volume for $m_\pi \leq 500$ MeV and $r_0 = 0.50$ fm.

very last 100 MeV from the physical point does g_A^R rise to its final value. This phenomenon is not totally unexpected, from general arguments [28] and from ChEFT [10, 29, 30]. Near the chiral limit ChEFT predicts, following the notation of [10],

$$\begin{aligned}
g_A^R(m_\pi) = & g_A^0 - \frac{g_A^{0\ 3}}{16\pi^2 f_0^2} m_\pi^2 + 4 [B_9^r(m_{\pi\text{phys}}) - 2g_A^0 B_{20}^r(m_{\pi\text{phys}})] m_\pi^2 \\
& - \frac{g_A^{0\ 3} - g_A^0/2}{4\pi^2 f_0^2} m_\pi^2 \ln(m_\pi/m_{\pi\text{phys}}) + O(m_\pi^3) .
\end{aligned} \tag{15}$$

To this order, both sets of chiral expansions, [10, 29] and [30], are equivalent with $B_9 = d_{16}$ and $B_{20} = d_{28}$. In (15) we have chosen $\lambda = m_{\pi\text{phys}}$ (λ being the scale parameter of the dimensional regularization). The coupling B_{20}^r cannot be observed independently of B_9^r . Taking $B_{20}^r(m_{\pi\text{phys}}) \equiv 0$, the preferred value of B_9^r is [31] $B_9^r(m_{\pi\text{phys}}) = (-1.4 \pm 1.2) \text{ GeV}^{-2}$. A fit of the leading order chiral formula (15) to the data points in Fig. 4 is shown by the shaded area. The fit gives $g_A^0 = 1.26(7)$ and $B_9^r(m_{\pi\text{phys}}) = (-2.1 \pm 1.0) \text{ GeV}^{-2}$. We do not see any scaling violations in the region where we have results at multiple lattice spacings, i.e. $m_\pi \gtrsim 250$ MeV. However, below that region we cannot draw any further conclusions.

Our results for f_π^R are plotted in Fig. 5. Again, no extrapolation to the physical point is needed, where we obtain from our lightest simulation point

$$f_\pi^R = 89.7 \pm 1.5 \pm 1.8 \text{ MeV} , \tag{16}$$

using $r_0 = 0.50(1)$ fm. The second error in eq. (16) is due to the error on r_0 . In the case of f_π^R we do not see any scaling violations either.

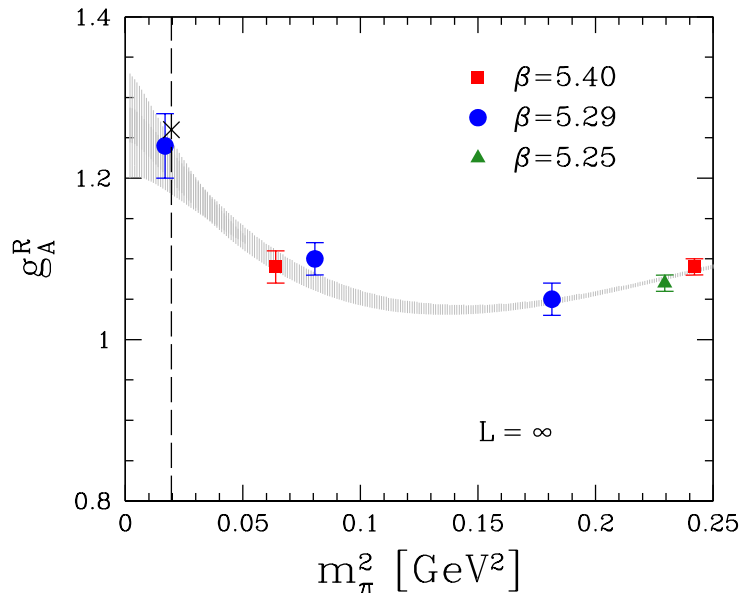


FIG. 4: The renormalized axial charge g_A^R in the infinite volume plotted against $m_\pi^2(\infty)$, together with the experimental value $g_A = 1.27$ (\times). The shaded area shows the fit of eq. (15) to the data.

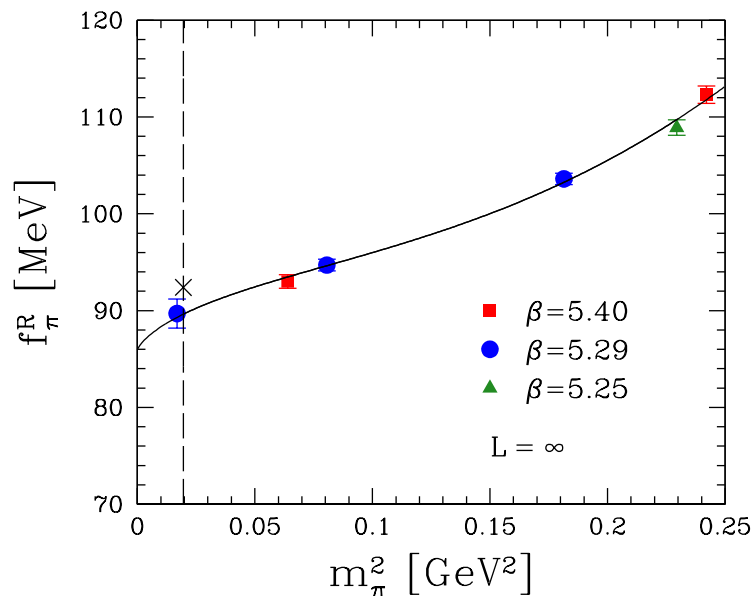


FIG. 5: The renormalized pion decay constant f_π^R in the infinite volume plotted against $m_\pi^2(\infty)$, together with the experimental value $f_\pi = 92.2$ MeV (\times). The curve shows a fit of eq. (17) to the data.

Instead of taking f_π^R from the entry at the lowest pion mass, eq. (16), it might be a better idea to include the adjacent data points in the analysis as well and fit the data by a chiral ansatz [24],

$$f_\pi^R = f_0 \left[1 - \frac{m_\pi^2}{16\pi^2 f_\pi^R{}^2} \ln(\Lambda_4^2/m_\pi^2) \right]^{-1} + A m_\pi^4. \quad (17)$$

The result of the fit is shown in Fig. 5. At the physical point we obtain the result

$$f_\pi^R = 89.6 \pm 1.1 \pm 1.8 \text{ MeV}, \quad (18)$$

which is fully consistent with the number in eq. (16). The main effect is that the statistical error has reduced by 30%. In the chiral limit we obtain $f_0 = 86(1) \text{ MeV}$, which agrees with the number used in the finite size correction formulae. A fit of the chiral ansatz (17) to the lowest four data points with $A = 0$ gives the low-energy constant

$$\bar{l}_4 = \ln(\Lambda_4^2/m_{\pi\text{phys}}^2) = 4.2 \pm 0.1. \quad (19)$$

Though eqs. (5) and (6) describe the finite size corrections very well, it should be noted that other choices of the pion decay constant (for example f_π instead of f_0) are possible. There is also some ambiguity in the determination of the renormalization constant Z_A [8]. Finite size corrections and uncertainties of Z_A can be evaded by considering the ratio g_A/f_π . In Fig. 6 we plot the ratio g_A/f_π for our (raw) data points listed in Table I, restricting ourselves to pion masses $m_\pi \leq 750 \text{ MeV}$ and again taking $r_0 = 0.50(1) \text{ fm}$ to set the scale. If we have more than one volume at a given κ value, we show the result of the largest volume. The data points for all three β values lie nicely on a universal curve. The lowest pion mass in Fig. 6 is 157 MeV (as opposed to 130 MeV in the infinite volume).

The leading order chiral expansion of g_A/f_π (in the infinite volume) can be cast in the form [10, 24, 29]

$$\frac{g_A}{f_\pi} = A + B m_\pi^2 + C m_\pi^2 \ln m_\pi^2 + D m_\pi^4. \quad (20)$$

We have fitted eq. (20) to the data points in Fig. 5. The result is shown by the solid curve. At the physical point this gives

$$\frac{g_A}{f_\pi} = 13.95 \pm 0.71 \pm 0.30 \text{ GeV}^{-1}. \quad (21)$$

Again, the second error is due to the error on r_0 . Multiplying the ratio (21) by the physical value of f_π , $f_\pi = 92.2 \text{ MeV}$, we then obtain

$$g_A^R = 1.29 \pm 0.05 \pm 0.03. \quad (22)$$

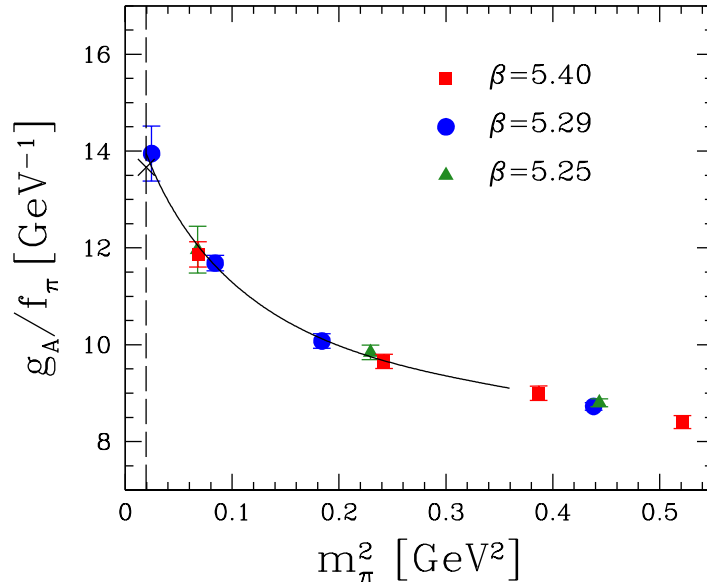


FIG. 6: The ratio g_A/f_π , together with the experimental value (\times). The curve shows a fit of eq. (20) to the data.

This result is in agreement with the direct calculation of g_A^R given in eq. (14), which involved extrapolation of g_A to the infinite volume and nonperturbative renormalization.

In Fig. 6 we have set the scale by $r_0 = 0.50(1)$ fm. Alternatively, we could have set the scale by the physical value of f_π . That would give the value

$$g_A^R = 1.27 \pm 0.05. \quad (23)$$

Acknowledgement

The gauge configurations were generated using the BQCD code [32] on the BlueGene/L and BlueGene/P at NIC (Jülich), the BlueGene/L at EPCC (Edinburgh), the SGI ICE 8200 at HLRN (Berlin and Hannover), and on QPACE. The Chroma software library [33] was used in the data analysis. This work would not have been possible without the input of Dirk Pleiter. We thank him most sincerely for his contributions. Benjamin Gläfle computed some two- and three-point functions for us, which we gratefully acknowledge. This work has been supported partly by the EU grants 283286 (HadronPhysics3) and 227431 (HadronPhysics2), and by the DFG under contract SFB/TR 55 (Hadron Physics from Lattice QCD). JMZ is

supported by the Australian Research Council grant FT100100005. We thank all funding agencies.

-
- [1] R. G. Edwards, G. T. Fleming, Ph. Hägler, J. W. Negele, K. Orginos, A. V. Pochinsky, D. B. Renner, D. G. Richards and W. Schroers, *Phys. Rev. Lett.* **96**, 052001 (2006) [hep-lat/0510062].
 - [2] T. Yamazaki, Y. Aoki, T. Blum, H.-W. Lin, M.-F. Lin, S. Ohta, S. Sasaki, R. J. Tweedie and J. M. Zanotti, *Phys. Rev. Lett.* **100**, 171602 (2008) [arXiv:0801.4016 [hep-lat]].
 - [3] C. Alexandrou, M. Brinet, J. Carbonell, M. Constantinou, P. A. Harraud, P. Guichon, K. Jansen, T. Korzec and M. Papinutto, *Phys. Rev. D* **83**, 045010 (2011) [arXiv:1012.0857 [hep-lat]].
 - [4] S. Capitani, M. Della Morte, G. von Hippel, B. Jäger, A. Jüttner, B. Knippschild, H. B. Meyer and H. Wittig, *Phys. Rev. D* **86**, 074502 (2012) [arXiv:1205.0180 [hep-lat]].
 - [5] For reviews see: H.-W. Lin, arXiv:1112.2435 [hep-lat]; H.-W. Lin, *PoS LATTICE 2012*, 013 (2012) [arXiv:1212.6849 [hep-lat]].
 - [6] G. Martinelli, C. Pittori, C. T. Sachrajda, M. Testa and A. Vladikas, *Nucl. Phys. B* **445**, 81 (1995) [hep-lat/9411010];
M. Göckeler, R. Horsley, H. Oelrich, H. Perlt, D. Petters, P. E. L. Rakow, A. Schäfer, G. Schierholz and A. Schiller, *Nucl. Phys. B* **544**, 699 (1999) [hep-lat/9807044].
 - [7] M. Göckeler, R. Horsley, Y. Nakamura, H. Perlt, D. Pleiter, P. E. L. Rakow, A. Schäfer, G. Schierholz, A. Schiller, H. Stüben and J. M. Zanotti, *Phys. Rev. D* **82**, 114511 (2010) [arXiv:1003.5756 [hep-lat]].
 - [8] M. Constantinou, M. Costa, M. Göckeler, R. Horsley, H. Panagopoulos, H. Perlt, P. E. L. Rakow, G. Schierholz and A. Schiller, *PoS LATTICE 2012*, 239 (2012) arXiv:1210.7737 [hep-lat].
 - [9] S. R. Beane and M. J. Savage, *Phys. Rev. D* **70**, 074029 (2004) [hep-ph/0404131].
 - [10] A. Ali Khan, M. Göckeler, P. Hägler, T. R. Hemmert, R. Horsley, D. Pleiter, P. E. L. Rakow, A. Schäfer, G. Schierholz, T. Wollenweber and J. M. Zanotti, *Phys. Rev. D* **74**, 094508 (2006) [hep-lat/0603028].
 - [11] G. Colangelo, S. Dürr and C. Haefeli, *Nucl. Phys. B* **721**, 136 (2005) [hep-lat/0503014].

- [12] S. Collins, M. Göckeler, Ph. Hägler, T. Hemmert, R. Horsley, Y. Nakamura, A. Nobile, H. Perlt, D. Pleiter, P. E. L. Rakow, A. Schäfer, G. Schierholz, A. Sternbeck, H. Stüben, F. Winter and J. M. Zanotti, PoS LATTICE **2010**, 153 (2010) [arXiv:1101.2326 [hep-lat]].
- [13] G. S. Bali, P. C. Bruns, S. Collins, M. Deka, B. Gläbke, M. Göckeler, L. Greil, T. R. Hemmert, R. Horsley, J. Najjar, Y. Nakamura, A. Nobile, D. Pleiter, P. E. L. Rakow, A. Schäfer, R. Schiel, G. Schierholz, A. Sternbeck and J. M. Zanotti, Nucl. Phys. B **866**, 1 (2013) [arXiv:1206.7034 [hep-lat]].
- [14] M. Della Morte, R. Hoffmann and R. Sommer, JHEP **0503**, 029 (2005) [hep-lat/0503003].
- [15] M. Göckeler, R. Horsley, E. -M. Ilgenfritz, H. Perlt, P. E. L. Rakow, G. Schierholz and A. Schiller, Phys. Rev. D **53**, 2317 (1996) [hep-lat/9508004].
- [16] S. Capitani, M. Göckeler, R. Horsley, B. Klaus, H. Oelrich, H. Perlt, D. Petters, D. Pleiter, P. E. L. Rakow, G. Schierholz, A. Schiller and P. Stephenson, Nucl. Phys. Proc. Suppl. **73**, 294 (1999) [hep-lat/9809172].
- [17] B. J. Owen, J. Dragos, W. Kamleh, D. B. Leinweber, M. S. Mahbub, B. J. Menadue and J. M. Zanotti, arXiv:1212.4668 [hep-lat].
- [18] M. Göckeler, R. Horsley, D. Pleiter, P. E. L. Rakow, G. Schierholz, W. Schroers, H. Stüben and J. M. Zanotti, PoS LAT **2005**, 063 (2006) [hep-lat/0509196].
- [19] N. L. Hall, A. W. Thomas, R. D. Young and J. M. Zanotti, arXiv:1205.1608 [hep-lat].
- [20] T. A. Gail and T. R. Hemmert, Eur. Phys. J. A **28**, 91 (2006) [nucl-th/0512082].
- [21] H. Leutwyler, Phys. Lett. B **189**, 197 (1987).
- [22] P. Hasenfratz and F. Niedermayer, Z. Phys. B **92**, 91 (1993) [arXiv:hep-lat/9212022].
- [23] P. Hasenfratz, Nucl. Phys. B **828**, 201 (2010) [arXiv:0909.3419 [hep-th]].
- [24] G. Colangelo, J. Gasser and H. Leutwyler, Nucl. Phys. B **603**, 125 (2001) [arXiv:hep-ph/0103088].
- [25] W. Bietenholz, M. Göckeler, R. Horsley, Y. Nakamura, D. Pleiter, P. E. L. Rakow, G. Schierholz and J. M. Zanotti, Phys. Lett. B **687**, 410 (2010) [arXiv:1002.1696 [hep-lat]].
- [26] G. Colangelo and S. Dürr, Eur. Phys. J. C **33**, 543 (2004) [hep-lat/0311023].
- [27] S. Sint and P. Weisz, Nucl. Phys. B **502**, 251 (1997) [hep-lat/9704001].
- [28] R. L. Jaffe, Phys. Lett. B **529**, 105 (2002) [hep-ph/0108015].
- [29] M. Procura, B. U. Musch, T. R. Hemmert and W. Weise, Phys. Rev. D **75**, 014503 (2007) [hep-lat/0610105].

- [30] V. Bernard and U. -G. Meissner, Phys. Lett. B **639**, 278 (2006) [hep-lat/0605010].
- [31] T. R. Hemmert, M. Procura and W. Weise, Phys. Rev. D **68**, 075009 (2003) [hep-lat/0303002].
- [32] Y. Nakamura and H. Stüben, PoS LATTICE **2010**, 040 (2010) [arXiv:1011.0199 [hep-lat]].
- [33] R. G. Edwards and B. Joó [SciDAC and LHPC and UKQCD Collaborations], Nucl. Phys. Proc. Suppl. **140**, 832 (2005) [hep-lat/0409003].